ACS APPLIED MATERIALS & INTERFACES

Research Article

www.acsami.org

Centrifugal Spinning: An Alternative for Large Scale Production of Silicon–Carbon Composite Nanofibers for Lithium Ion Battery Anodes

Rocío Nava,*[,†] Lee Cremar,[‡] Victor Agubra,[‡] Jennifer Sánchez,[‡] Mataz Alcoutlabi,[‡] and Karen Lozano[‡]

[†]Instituto de Energías Renovables, Universidad Nacional Autónoma de México, Privada Xochicalco s/n, Temixco Morelos 62580, México

[‡]Department of Mechanical Engineering, University of Texas Rio Grande Valley, 1201 West University Drive, Edinburg, Texas 78539, United States

ABSTRACT: Composites made of silicon nanostructures in carbon matrixes are promising materials for anodes in Li ion batteries given the synergistic storage capacity of silicon combined with the chemical stability and electrical conductivity of carbonaceous materials. This work presents the development of Si/C composite fine fiber mats produced by carbonization of poly(vinyl alcohol) (PVA)/Si composites. PVA has a high carbon content (ca. 54.5%) and, being water-soluble, it promotes the development of environmentally friendly materials. Si nanoparticles were dispersed in PVA solutions and transformed into fine fibers using a centrifugal spinning technique given its potential for large scale production. The Si/PVA fibers mats were then subjected to dehydration by exposing them to sulfuric acid vapor. The dehydration improved the thermal and chemical stability of the PVA matrix, allowing further carbonization at 800 °C. The resulting Si/C composite fibers produced binder-free anodes for lithium ion batteries that delivered specific discharge and charge capacities of 952 mA h g^{-1} and 862 mA g^{-1}, respectively, with a Columbic efficiency of 99% after 50 cycles.

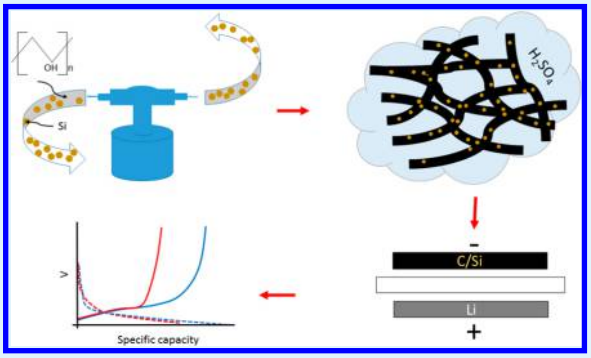

KEYWORDS: *silicon, carbon, poly(vinyl alcohol), centrifugal spinning, lithium batteries, nanofibers*

1. INTRODUCTION

Silicon is the most promising material for anodes in Li ion batteries due to its high theoretical storage capacity, 4200 mA h g^{-1}, and low discharge potential (below 0.5 V).[1] However, bulk Si anodes experience extreme volume changes, >300%, during the charge and discharge of Li ions. This results in pulverization of the bulk Si which eventually leads to the loss of electrical contact after a few cycles of operation. On the other hand, Si nanostructures are more flexible than bulk Si because they have empty spaces to accommodate volume changes and release mechanical stresses.[2,3] Nevertheless, extending the life cycle of Si nanostructure-based anodes is a complex task because there are several other factors that play a role in the overall capacity, for example, the formation of a solid electrolyte interface (SEI) and the growth of Li metal on the anode, among others.[4] The SEI layer is formed on the Si anode by products arising from the electrochemical degradation of the electrolyte, and it has a significant impact on the battery performance. The SEI passivates the anode to prevent further electrolyte decomposition, but due to the continuous volume changes of the anode, it peels and grows again, therefore reducing the available Li ions in the electrolyte and battery capacity after each cycle.[5] On the other hand, graphite anodes used in commercial Li ion batteries have lower storage capacity (372 mA h g^{-1}) but higher ion diffusion, chemical stability, and electrical conductivity and longer life cycle than that of Si anodes. Alternatively, composites containing Si nanostructures within graphite matrixes or other carbonaceous materials (Si/C composites) have shown improvements in the overall electrochemical performance of the anode by combining the properties of both materials, specifically the electrical contact and chemical stability.[6−13]

The development of Si/C composite fibers can facilitate the Li ion exchange between anode and electrolyte due to its large surface area. A wide variety of materials such as polymers, composites, and ceramics have been produced as fine fibers by the electrospinning method.[14,15] In particular, carbon[16−18] and Si/C[6−13] fibers produced by electrospinning have shown high performance as lithium battery anodes. However, the electrospinning technique has intrinsic restrictions associated with the technology itself such as dependence on the dielectric properties of the solution to be spun, the electric field strength, and mainly a low yield production (<0.3 g per hour). On the other hand, centrifugal spinning is a less known technique used

Received: May 20, 2016
Accepted: October 12, 2016
Published: October 12, 2016

DOI: 10.1021/acsami.6b06051
ACS Appl. Mater. Interfaces 2016, 8, 29365−29372

to produce fibers but with significantly higher yield than electrospinning (1 g/min for lab scale systems and hundreds of meters per minute with adjustable grams per square meter for the industrial systems). In the centrifugal spinning process, also known as forcespinning, a liquid material (in solution or melted) is deposited in a spinneret which has either fine needles (in the case of lab scale systems) or small nozzles (industrial units). The spinneret is then rotated at high speeds (usually in the range of 4000−10 000 rpm), and the material is centrifugally forced through the designed orifices, ejected, and continues its elongation/extensional flow as the solvent evaporates or melt cools until deposition on a collector. Due to its nature, the production of fibers by centrifugal spinning depends on the viscoelastic nature of the material to be spun, the rotational speed, and the spinneret design, being totally independent of the electrical properties. This process therefore broadens the spectrum of materials that can be converted into fibers and gives an alternative for large scale production at low cost.[19]

The polymer precursor used to produce the carbon matrix also plays an important role in the performance and cost of the Si/C composite fibers. Si/C fibers have been commonly produced by converting a polymer solution containing the Si nanostructure into fibers and then subjecting the developed fibers to a heat treatment process for complete carbonization. Polyacrilonitrile (PAN) is commonly used because of its high carbon content and mechanical properties. PAN-based carbon fibers have been widely adopted for several high-tech applications though the high cost of the PAN has prevented the widespread use of carbon fibers for a variety of applications. Poly(vinyl alcohol) (PVA) is a low cost and water-soluble polymer with also a high carbon content, though not commonly used as a precursor of carbon fibers. PVA usually melts at a relatively low temperature, causing fibers to collapse into each other or decompose before carbonization is completed. This study presents the development of Si nanostructure-reinforced PVA fibers, which are subjected to an efficient carbonization process to obtain Si/C composite fibers. A key step in the process is that the precursor PVA-based fibers are chemically stabilized by exposure to sulfuric acid vapor and subsequent carbonization to form Si/C fibers that are then used as anodes for Li ion batteries.

2. EXPERIMENTAL SECTION

2.1. Fiber Development. PVA (Aldrich, MW 85 000−124 000) was dissolved in distilled water (14% w/w) by magnetic stirring at 70 °C for 5 h. In a separate procedure, Si nanoparticles (U.S. Nanomaterials) of 20−30 nm were also mixed in distilled water at a concentration of 19% (w/w) and sonicated for 4 h. The PVA solution and Si nanoparticle suspension were subsequently mixed and homogenized at 5000 rpm for 2 h. The weight ratio of PVA to Si nanoparticles was 2:1. The composite precursor was then subjected to a centrifugal spinning process in a lab scale Cyclone L-1000 M from Fiberio Technology Corporation to produce fine fibers. The spinneret was equipped with 30-gauge regular bevel needles (Beckett-Dickerson). One milliliter of PVA/Si nanoparticle solution was deposited in the spinneret and rotated at 5000 rpm during 5 min to produce fine fibers. The fibers were then collected, and the process was repeated 10 times to form a mat. A free-standing Si nanoparticle-reinforced PVA fiber mat was obtained. The mat was partially carbonized by exposure to acid vapor produced by heating sulfuric acid (concentration of 98%, purchased from Sigma-Aldrich and used as received) to 250 °C for approximately 2 h in a semiclosed container. During this process, the mat became blackish and insoluble in water. The mats were then washed with distilled water to remove residual traces of H_2SO_4 and dried in air at room temperature. Full carbonization of the mat was completed in a tube furnace under a nitrogen atmosphere at 800 °C with a ramping of 10 °C/min and held at the final temperature for 30 min.

A control sample of pure carbon fiber membranes was also developed by dissolving PVA in distilled water (10% w/w) at 70 °C with magnetic stirring for 5 h. PVA fibers were produced by centrifugally spinning the solution at 6000 rpm and transformed into carbon fiber as described above.

2.2. Cell Assembly. Electrochemical experiments were performed using coin-type half-cells, one with the Si/C composite fibers and another with pure carbon fibers as the working electrodes. Lithium metal foil was used as the reference electrode and a Celgard membrane as the separator. The assembly of the cells was performed in a glovebox (MBraun, Stratham, NH) filled with high purity argon (oxygen and moisture content <0.5 ppm). Given that the Si/C composite and carbon mats were flexible and electrically conductive, they were assembled directly into cells of 1/2-in. diameter without any binder, additive, or current collector (i.e., the base CR2032 cell acted as current collector). The average weight of Si/C and C anodes was 3.67 mg and 3.38 mg, respectively. The electrolyte used was a 1 M $LiPF_6$ solution in ethylene carbonate (EC)/dimethyl carbonate (DMC) (1:1 v/v).

2.3. Characterization. The morphology of the Si/C fiber mat was examined using a field-emission scanning electron microscope (FE-SEM; Sigma VP Carl Zeiss, Germany). For the X-ray diffraction analysis, a Bruker AXS D8 diffractometer was utilized with scans performed in the 2θ = 15° to 80° range. TGA was recorded with a thermal analyzer Q600 from room temperature to 800 °C, with a heating rate of 10 °C/min. FT-IR spectra were recorded with a Spectrum GX PerkinElmer system. The states of the carbon structures and Si in the fibers were determined by X-ray photoelectron spectroscopy (XPS) with a Thermoscientific K-α XPS surface analysis instrument using a microfocused monochromatic Al K-α X-ray source. The electrochemical performance was evaluated by carrying out galvanostatic charge−discharge experiments at a current density of 100 mA g^{-1} between 0.05 and 3.00 V. The specific charge/discharge capacities were calculated based on the mass of the flexible fiber electrodes. The cyclic voltammetry and impedance were evaluated using an electrochemical impedance spectroscope (Autolab 128N) with a scan rate of 0.05 mV/s between 0 and 3 V, and frequency of 0.1 Hz and 1 MHz.

3. RESULTS AND DISCUSSION

Figure 1 shows the produced composite fiber systems. Parts a and b correspond to the PVA/Si composite nanoparticle fibers within the Cyclone and the collected fibers as free-standing nonwoven mats, respectively. Parts c and d show the scanning electron (SEM) and the scanning tunneling electron (STM) images of the fully carbonized Si/C composite fibers, correspondingly. Images are shown at the same magnification (50k×) for comparison. As observed, there is a high Si nanoparticle content with the existence of some agglomerates in the fibers, therefore a heterogeneous dispersion of Si nanoparticles. It is also clearly seen that the Si nanoparticles were well embedded within a dense carbon matrix without the need for surfactants to improve wettability of the Si nanoparticles to the PVA. As shown in Figure 1c and 1d, the fiber structure is preserved after heat treatment at 800 °C due to the pretreatment of the PVA with sulfuric acid vapor. Usually PVA fibers reported in literature are carbonized below 650 °C to avoid decomposition and melting.[10,12] Figure 2 shows the TGA results of PVA fibers (dash blue line), PVA/Si composite fibers (red dot line), partially carbonized fiber Si/C composite with sulfuric acid vapor (black solid line), and the fully carbonized Si/C fibers after the sulfuric acid and heat treatments (solid gray line). An almost total degradation of

DOI: 10.1021/acsami.6b06051
ACS Appl. Mater. Interfaces 2016, 8, 29365−29372

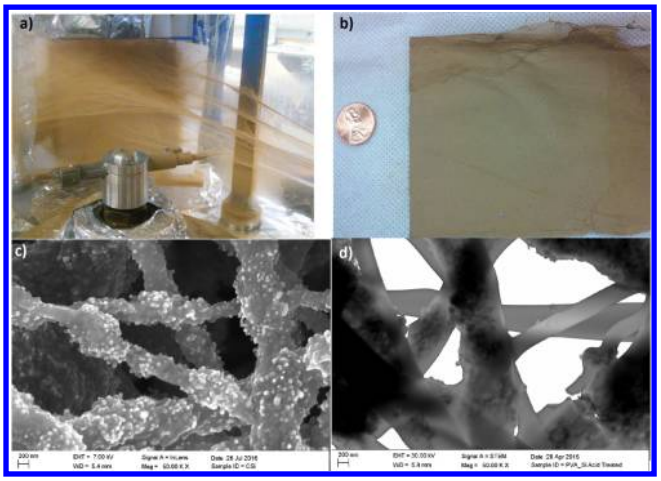

Figure 1. (a) Si nanoparticles/PVA fibers while being developed, (b) Si/PVA fiber nonwoven mats, (c) scanning electron micrograph of the developed mats, and (d) scanning tunneling micrographs of the fully carbonized Si/C fibers.

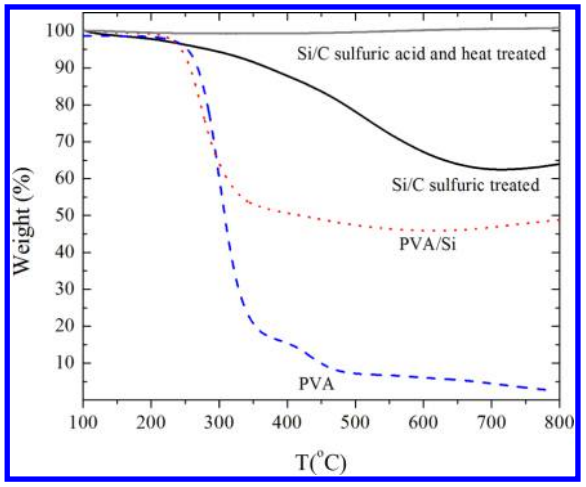

Figure 2. TGA of the developed fiber composites: Pure PVA fibers (blue dashed line) as reference, PVA/Si composite fibers (red dotted line), Si/C composite fibers after the sulfuric acid treatment (black solid line), and Si/C composite fiber after the sulfuric acid and heat treatment processes (grey solid line).

pure PVA fibers at 800 °C is clearly shown. The plot corresponding to PVA/Si composite fibers (without sulfuric acid and heat treatments) shows approximately a 42% weight content of silicon nanoparticles in the PVA matrix. As this sample was obtained from a solution with a ratio of 2:1 (PVA to Si), this result was therefore unexpected. Careful analysis of the sample preparation procedure revealed that during homogenization of the PVA/Si solution, a PVA-rich film had formed in the generator probe, therefore considerably decreasing the PVA concentration. The TGA of the Si/C fiber treated with sulfuric acid vapor (solid black line) shows a reduction in mass of 27% when heated to around 700 °C; as some organic components are evaporated, the concentration of Si in the sample increases further. At higher temperature, there is an increase in the mass due to silicon oxidation. The heating of the sample for the TGA is similar to the heat treatment applied to fully carbonize the fibers, such that around the same mass loss of the organic matrix is expected. It can be concluded that the concentration of Si nanoparticles in the fully carbonized Si/C composite is close to 50%, and this sample is thermally stable in the temperature range applied (solid gray line).

Figure 3 shows the EDS spectrum of the final Si/C composite fibers. The element concentration is Si, C, and O

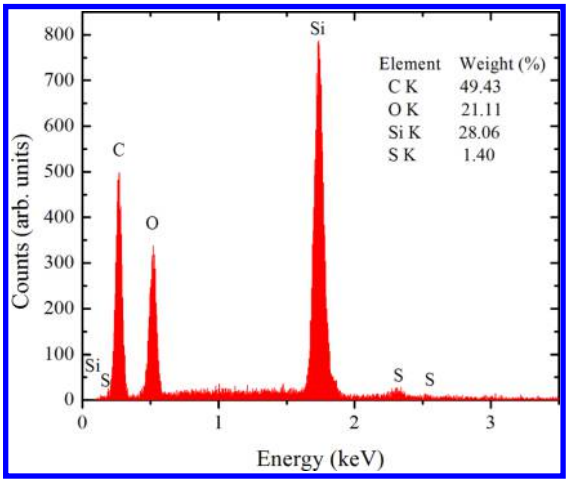

Figure 3. EDS spectra of the Si/C composite fiber after the sulfuric acid and heat treatment processes.

with 28%, 50%, and 21%, respectively. Small residues of sulfur were detected in basically negligible quantities given the sulfuric acid dehydration treatment. Because oxygen can bind to carbon and silicon, further analysis was required to identify the oxidized compounds. Figure 4 shows the XPS analysis of the Si/C fibers obtained after the sulfuric acid and heat treatments. The survey analysis shown in Figure 4a displays several peaks corresponding to the O(1s), C(1s), Si(2s), and Si(2p) states. The deconvoluted C(1s) spectra, shown in Figure 4b, clearly exhibit a peak at 284.5 eV corresponding to sp^2-hybridized C atoms present in graphite and polyene type structures. The analysis of the deconvoluted Si(2p) state, Figure 4c, shows a large peak for silicon dioxide at 103.5 eV and a small peak for Si at 99.1 eV, respectively. The deconvoluted spectra of the O(1s) state also indicate that oxygen is bonded to Si on the surface of the particles. The FTIR spectra of pure PVA fibers, Si/C composite fibers after sulfuric acid treatment, and fully carbonized Si/C composite fibers (after sulfuric acid and heat treatment at 800 °C) are shown in Figures 5, parts a, b, and c, respectively. The FTIR spectrum, shown in Figure 5a for the pure PVA fibers, is used as a reference to clearly identify the reaction products when exposed to sulfuric acid. Sulfuric acid vapor reacted with the PVA matrix to cause dehydration and oxidation, which resulted in removal of the water-bearing groups;[20] see regions I and II of Figure 5a and 5b corresponding to the O−H and C−H stretch, respectively. As a result, the Si nanoparticle-reinforced PVA composite mat became blackish and insoluble when washed with water given the formation of polyene type structures (around 1642 cm^{-1} in Figure 5b). As observed in Figure 5c, the heat treatment at 800 °C completed the dehydration of the PVA matrix and reduced the available C═C and C═O bonds. Si−O−Si bonds were also detected, but the Si−Si bond at 611 cm^{-1} was out of the range of detection of the equipment. The carbon structures produced by exposing PVA to sulfuric acid vapor further prevent decomposition of the fibers as they are heated to 800 °C to improve their electrical conductivity. The dehydration

DOI: 10.1021/acsami.6b06051
ACS Appl. Mater. Interfaces 2016, 8, 29365−29372

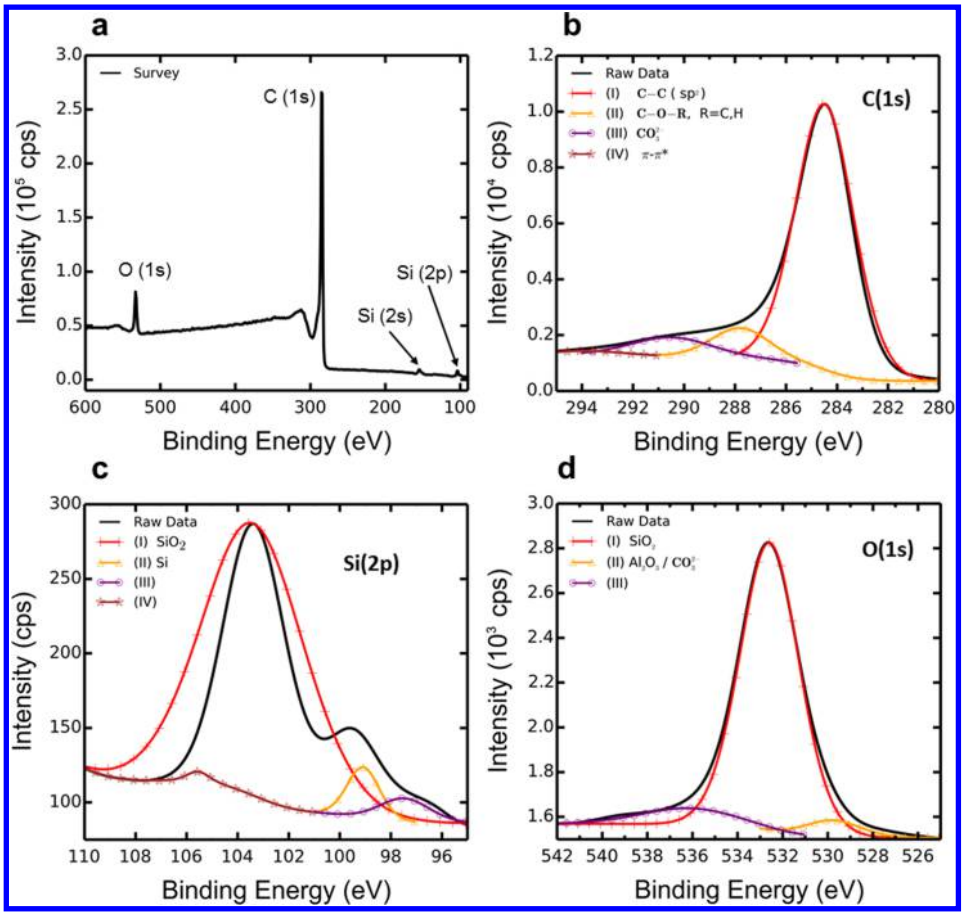

Figure 4. XPS analysis of the final Si/C fiber composite: (a) survey spectrum, and (b) C (1s), (c) Si (2p), and (d) O (1s) deconvolution peaks with their corresponding states.

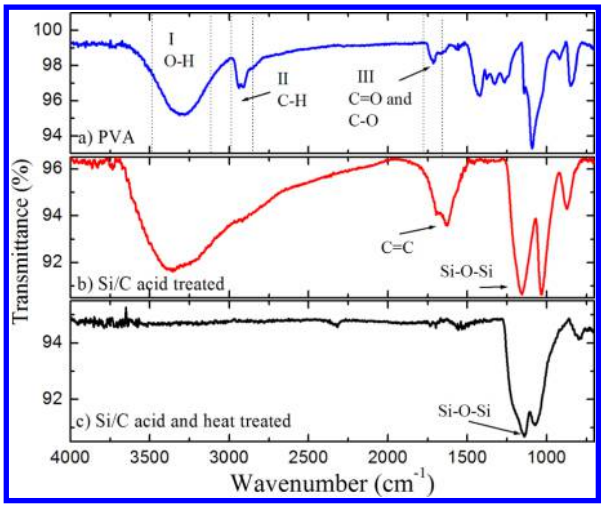

Figure 5. FTIR spectra of (a) pure PVA fibers, (b) Si/C fiber composite after exposure to sulfuric acid vapor, and (c) Si/C fiber composite after sulfuric and heat treatment processes.

process of the PVA fibers with sulfuric acid vapor is similar to a previously reported method where iodine was used to form polyene type carbon structures[21] but with the advantage that residuals of sulfuric acid in the fibers are relatively easily removed with water.

It is known that sulfuric acid slowly oxidizes powdered silicon, and that silicon oxide can react with a boiling solution of concentrated sulfuric acid to produce silicon dioxide, sulfur dioxide, and water.[22] Herein, due to the relatively short exposure time (2 h) of the Si nanoparticles to the sulfuric acid vapor, required to carbonize the PVA matrix, a slight oxidation of Si was expected and confirmed by XRD analysis. Figure 6 shows the XRD pattern of (a) PVA-Si composite fibers, (b) Si/C composite produced by the sulfuric acid vapor treatment, and (c) the final Si/C composite fibers produced by heating at 800 °C in a nitrogen atmosphere after the sulfuric acid vapor treatment. The observed sharp peaks in the XRD pattern correspond to the Si nanoparticles in the fibers. It is evident

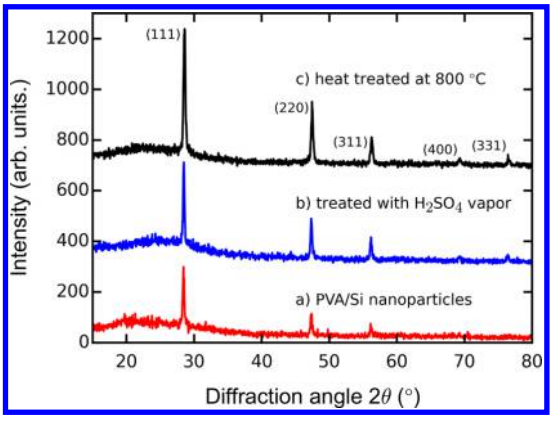

Figure 6. XRD pattern at each step of the process for production of Si/C fiber composite.

DOI: 10.1021/acsami.6b06051
ACS Appl. Mater. Interfaces 2016, 8, 29365−29372

that the Si crystalline structure is preserved during the full transformation process from the reinforced PVA-Si nanoparticles to the Si/C composite. The XRD pattern (Figure 6c) also shows a broad peak from 2θ = 15° to 30°, corresponding to an amorphous carbon matrix. The produced carbon matrix is flexible, see Figure 7, and electrically conductive, therefore

Figure 7. Flexible Si/C composite fiber mat used as binder-free anode.

ensuring electrical contact as a binder-free anode with the battery electrodes. These results show that the heat treatment at 800 °C preserved the fiber structure and enhanced the conductivity of the carbon matrix, although a higher temperature treatment is required to promote graphitization of the carbon matrix.

To better understand the alloying/dealloying process of the Si nanoparticles with the lithium ions, cyclic voltammetry of the negative electrode was carried out for the first three cycles at a scanning rate of 0.05 mV s^{-1} in the voltage range of 0−3 V. As shown in Figure 8, the CV scan for the Si/C composite

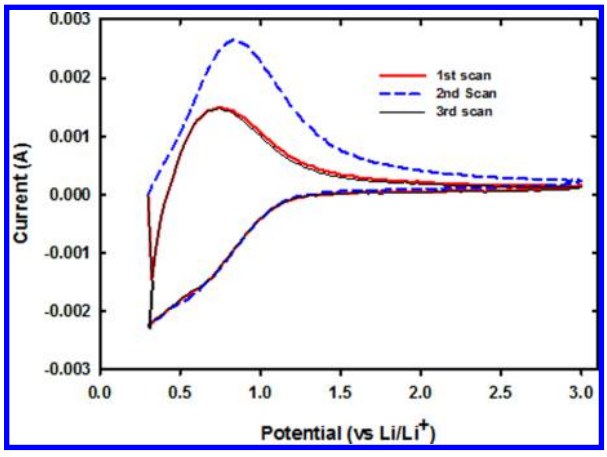

Figure 8. Cyclic voltammetry of Si/C composite electrode for the first three cycles at a scanning rate of 0.05 mV s^{-1} in the voltage range of 0−3.0 V.

electrode has one broad cathodic peak that appears between 0.2 to 0.4 V during the first cycle; this peak is attributed to alloying of the Si nanoparticles.[5] In the anodic scan, a broad peak was observed at potentials of ∼0.6 V, which shifted to 0.8 V (Li/Li^+) on the second scan and again returned to 0.6 V on the third scan. These potentials are often attributed to the electrolyte decomposition and the formation of a solid electrolyte interface (SEI) on the surface of the carbon matrix, as was previously observed in reports relating to carbon fiber fabrication from PVA.[10,20] The high anodic potential observed during the first and second scans is an indication of noninterference of the carbon matrix with the lithiation process of the Si nanoparticles.[15] The intensity of the anodic peak during the third scan indicates the transfer rate of Li^+ ions into the Si host and the reduction of the amorphous Li−Si alloy.

The storage/cycling performance for both the Si/C composite and the carbon fiber anodes at room temperature for the first 50 cycles was obtained. The charge/discharge cycling was performed between 0.05 and 3.0 V at a current density of 100 mA g^{-1}. In Figure 9 are shown the charge/

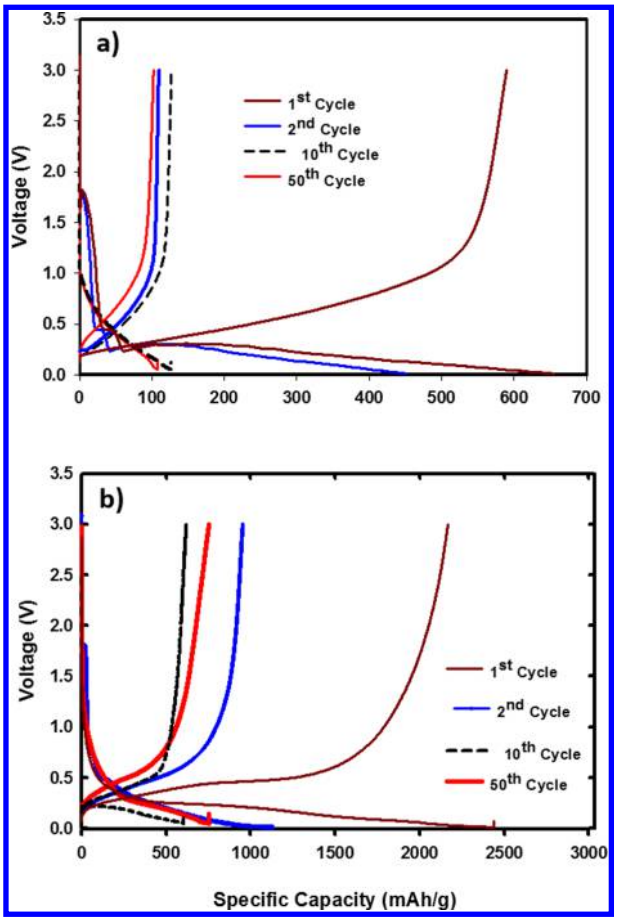

Figure 9. Charge/discharge curves for the 1st, 2nd, 10th, and 50th cycle of the (a) carbon and (b) Si/C composite anodes at a current density of 100 mA g^{-1}.

discharge curves of the (a) carbon fiber anode as reference and the (b) Si/C composite anodes. The discharge plateau observed at 0.4 V (vs Li/Li^+) for the Si/C composite anode is attributed to the initial decomposition reaction between the electrolyte and Li^+ ions to form the SEI layer.[23] In addition, another discharge voltage plateau appears at about 0.4−0.5 V vs Li/Li^+; it corresponds to the dealloying of the Si with Li ions. A comparison with the cyclic voltammetry results for the anodic scan corresponding to alloying potential, shown above in Figure 8, displays some slight discrepancy probably due to the charge contribution from sulfuric acid traces.

The cycling performance and Coulombic efficiency of both carbon and Si/C composite anodes are shown in Figure 10. It can be seen that for the first discharge cycle, the Si/C electrode

DOI: 10.1021/acsami.6b06051
ACS Appl. Mater. Interfaces 2016, 8, 29365−29372

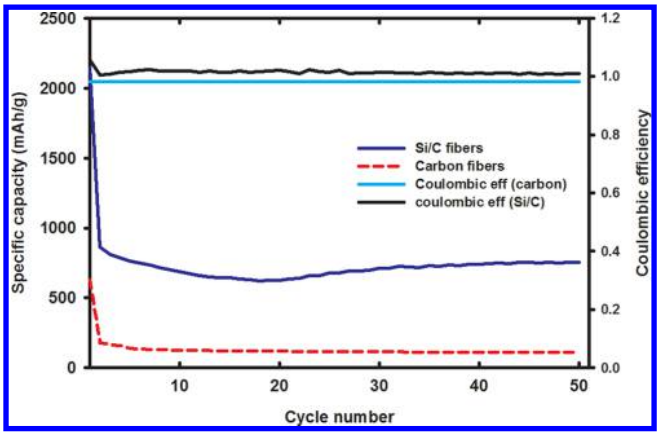

Figure 10. Cycling performance and columbic efficiency of carbon and Si/C composite electrodes.

recorded a capacity (Li insertion) of 2450 mA h g^{-1} compared to 650 mA h^{-1} for the carbon-based anode. The corresponding reversible charge capacities are about 2200 and 600 mA h g^{-1}, respectively. A considerable drop in the charge capacity for both the Si/C composite and carbon anodes can be observed. In the case of the Si/C composite fiber electrode, a drop from 2450 to 862 mA h g^{-1} was observed. For the carbon-based electrode, the capacity dropped from 625 to 178 mA h g^{-1}. The drastic drop in charge capacity for the Si/C composite anode is usually associated with the irreversible loss of Li^+ ions in the formation of the SEI layer and Li^+ ions trapped in the amorphous carbon matrix. However, the specific capacity of the Si/C composite electrode recovered from 625 mA h g^{-1} after the 20th cycle and steadily increased to 758 mA h g^{-1} beyond 50 cycles, while that of the carbon fiber anode remained flat. This behavior of the Si/C composite anode is often attributed to the gradual stabilization of the charge capacity of silicon in the composite.[10] Some reports showed a similar slight recovery in capacity upon cycling of Si/C-based anodes,[11,24−26] but a few of them explained this behavior.[11,26] In this work, the slight capacity recovery and stabilization of the Si/C composite fiber anode beyond the 20th cycle, shown in Figure 10, could be the result of an improved lithium diffusion in silicon due to pulverization of Si nanoparticles. Also, the cycling performance indicates that the Si/C composite electrode has a specific discharge and charge capacity of 952 and 862 mA g^{-1}, respectively, after the initial capacity drop, therefore resulting in an initial Columbic efficiency of 90.5%. Although the initial specific capacity of the carbon fiber anode was 625 mA h g^{-1}, which is greater than the theoretical capacity of graphite (372 mA h g^{-1}). Porous carbon and carbon fibers can have storage capacity larger than that of graphite due to their high surface area to volume ratio, and shorter distance for charge diffusion and electronic conduction.[16−18,27] A minor contribution to the initial large capacity of the carbon fiber anode could be due to the small traces of sulfur or sulfuric acid as detected. These carbon electrodes rapidly lost the initial high capacity to a steady value of 120 mA h g^{-1} over the 50 cycles (see Figures 9a and 10). The drop in storage capacity of amorphous carbon fiber anodes after the first discharge (Li^+ insertion) is usually attributed to the trapping of Li ions in the disordered sites.[28,29]

The relatively inherent high initial capacity of the Si/C and C anodes and the good cycle performance for at least 50 cycles is the result of a combination of several factors, such as the small size and large concentration of Si nanoparticles,[2] the chemical and thermal stability of the obtained carbon matrix, the free space between fibers available to accommodate the volume change produced during lithiation/delithiation,[27,28] and the high quality of the fibers produced using the centrifugal spinning process.

The Nyquist plots for the electrochemical impedance before and after cycling for the carbon and Si/C composite anodes are shown in Figure 11. This analysis was carried out to elucidate

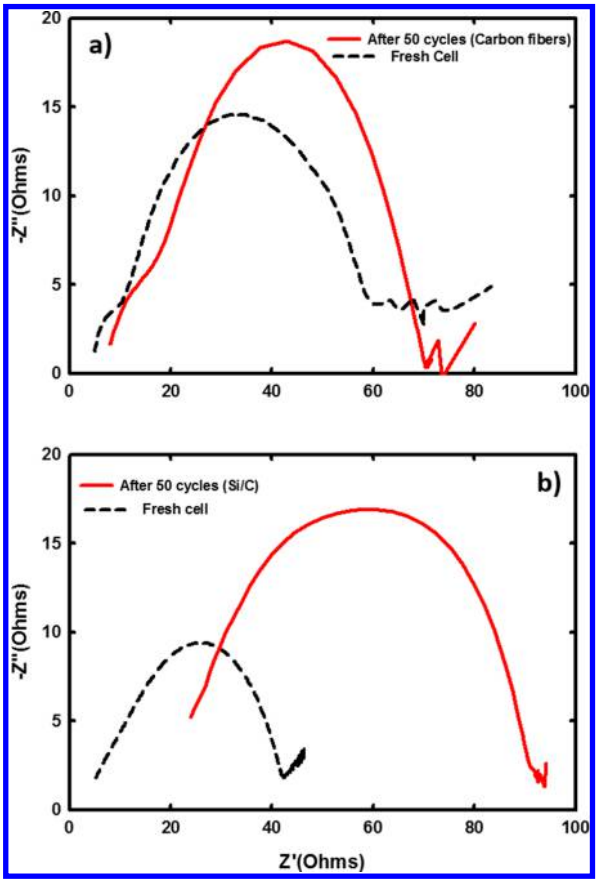

Figure 11. Nyquist plots for the electrochemical impedance before and after cycling for (a) carbon and (b) Si/C composite electrodes.

the associated electrochemical performance. The semicircles in the region from high to middle frequency range represent the initial interfacial resistance and charge-transfer resistance and clearly show a slight variation in impedance after 50 cycles for the carbon anode (Figure 11a). On the other hand, the Si/C composite electrode cell (Figure 11b) shows a remarkable increase in the cell impedance after 50 cycles which correlates with the drop in capacity displayed in Figure 9b. The increase in the diameter of the semicircle for both electrode types and the shift in the semicircle relative to the real *Z* axis clearly show an increase in the charge transfer resistance across the interface in the cell for both the Si/C and the carbon electrode. The increase in resistance at the electrode/electrolyte interface affects the kinetics of the Li ions at the interface, thereby negatively impacting the energy delivery of the cell. The rise in impedance after the 50 cycles is in agreement with the cycle performance results.

4. CONCLUSIONS

PVA, a water-soluble polymer, was used as the matrix for silicon nanoparticles. Fine fibers of PVA/Si nanoparticles were

DOI: 10.1021/acsami.6b06051
ACS Appl. Mater. Interfaces 2016, 8, 29365−29372

produced utilizing a centrifugal spinning process that has shown scalability for industrial purposes. The produced fibers were treated with sulfuric acid to remove the water-bearing groups in PVA and to promote the preservation of the fiber structure when heated up to 800 °C. Given that the Si/C fibers were flexible and electrically conductive, they were assembled directly into coin cells. The cycling performance of the Si/C shows a Columbic efficiency of 99% from above 20 cycles. Nyquist plots show an increase in the charge transfer resistance across the interface for both the Si/C and the C electrode with the cycling. The increase in resistance at the electrode/electrolyte interface affects the kinetics of Li ions, resulting in a negative impact on the delivery of the energy within the cell. Within the analyzed cycles (50), the fiber structure provides a buffering effect that mitigates volume changes associated with Si during the alloying/dealloying process. A graphitization of the carbon matrix, more homogeneous distribution of Si nanoparticles, and a porous carbonaceous matrix could help to extend the life cycle of these batteries.

AUTHOR INFORMATION

Corresponding Author

*E-mail: rnava@unam.mx.

Author Contributions

R. Nava and K. Lozano conducted the experiments and wrote the manuscript, L. Cremar conducted the carbonization process of the fibers and analysis. V. Agubra and M. Alcoutlabi performed the electrochemical analysis, and J. Sánchez produced the fiber mats. All authors reviewed the manuscript.

Notes

The authors declare no competing financial interest.

ACKNOWLEDGMENTS

The authors acknowledge support received from National Science Foundation under PREM grant DMR 1523577 and PAPIIT-UNAM IN117016. Also we acknowledge CONACYT by supporting the sabbatical leave of Dr. Nava at UTRGV, to Hilario Cortez for SEM images and EDS analysis, to Edgar Munoz for XPS analysis, and to Dr. Patricia Altuzar for TGA.

REFERENCES

(1) Boucamp, B. A.; Lesh, G. C.; Higgins, R. A. All-Solid Lithium Electrodes with Mixed-Conductor Matrix. *J. Electrochem. Soc.* **1981**, *128* (4), 725−729.

(2) Szczech, J. R.; Jin, S. Nanostructured Silicon for High Capacity Lithium Battery Anodes. *Energy Environ. Sci.* **2011**, *4*, 56−72.

(3) Wu, H.; Cui, Y. Designing Nanostructured Si Anodes for High Energy Lithium Ion Batteries. *Nano Today* **2012**, *7* (5), 414−429.

(4) Zhang, W. J. A Review of the Electrochemical Performance of Alloy Anodes for Lithium-Ion Batteries. *J. Power Sources* **2011**, *196* (1), 13−24.

(5) McDowell, M. T.; Lee, S. W.; Nix, W. D.; Cui, Y. 25th Anniversary Article: Understanding the Lithiation of Silicon and Other Alloying Anodes for Lithium-Ion Batteries. *Adv. Mater.* **2013**, *25* (36), 4966−4985.

(6) Wang, M. S.; Song, W. L.; Wang, J.; Fan, L. Z. Highly Uniform Silicon Nanoparticle/Porous Carbon Nanofiber Hybrids Towards Free-Standing High-Performance Anodes for Lithium-Ion batteries. *Carbon* **2015**, *82*, 337−345.

(7) Wang, M. S.; Song, W. L.; Fan, L. Z. Three-Dimensional Interconnected Network of Graphene-Wrapped Silicon/Carbon Nanofiber Hybrids for Binder-Free Anodes in Lithium-Ion Batteries. *ChemElectroChem* **2015**, *2*, 1699−1706.

(8) Zhou, X.; Wan, L. J.; Guo, Y. G. Electrospun Silicon Nanoparticles/Porous Carbon Hybrid Nanofibers for Lithium-Ion Batteries. *Small* **2013**, *9* (16), 2684−2688.

(9) Zhang, H.; Qin, X.; Wu, J.; He, Y. B.; Du, H.; Li, B.; Kang, F. Electrospun Core-Shell Silicon/Carbon Fibers with an Internal Honeycomb-Like Conductive Carbon Framework as Anode for Lithium Ion Batteries. *J. Mater. Chem. A* **2015**, *3*, 7112−7120.

(10) Fan, X.; Zou, L.; Zheng, Y. P.; Kang, F. Y.; Shen, W. C. Electrospinning Preparation of Nanosilicon/Disordered Carbon Composite as Anode Material in Li-Ion Battery. *Electrochem. Solid-State Lett.* **2009**, *12* (10), A199−A201.

(11) Fu, K.; Lu, Y.; Dirican, M.; Chen, C.; Yanilmaz, M.; Shi, Q.; Bradford, P. D.; Zhang, X. Chamber-Confined Silicon−carbon Nanofiber Composites for Prolonged Cycling Life of Li-Ion Batteries. *Nanoscale* **2014**, *6*, 7489−7495.

(12) Xu, Z. L.; Zhang, B.; Kim, J. K. Electrospun Carbon Nanofibers Anodes Containing Monodispersed Si Nanoparticles and Graphene Oxide with Exceptional High Rate Capacities. *Nano Energy* **2014**, *6*, 27−35.

(13) Wang, J.; Wang, C.; Zhu, Y.; Wu, N.; Tian, W. Electrochemical Stability of Optimized Si/C Composites Anode for Lithium-Ion Batteries. *Ionics* **2015**, *21*, 579−585.

(14) Pampal, E. S.; Stojanovska, E.; Simon, B.; Kilic, A. A Review of Nanofibrous Structures in Lithium Ion Batteries. *J. Power Sources* **2015**, *300*, 199−215.

(15) McCann, J. T.; Li, D.; Xia, Y. Electrospinning of Nanofibers with Core-Sheath, Hollow, or Porous Structures. *J. Mater. Chem.* **2005**, *15*, 735−738.

(16) Fatema, U. K.; Uddin, A. J.; Uemura, K.; Gotoh, Y. Fabrication of Carbon Fibers from Electrospun Poly(vinyl alcohol) Nanofibers. *Text. Res. J.* **2011**, *81* (7), 659−672.

(17) Kim, C.; Yang, K. S.; Kojima, M.; Yoshida, K.; Kim, Y. J.; Kim, Y. A.; Endo, M. Fabrication of Electrospinning-Derived Carbon Nanofiber Webs for the Anode Material of Lithium-Ion Secondary Batteries. *Adv. Funct. Mater.* **2006**, *16* (18), 2393−2397.

(18) Ji, L.; Lin, Z.; Medford, A. J.; Zhang, X. Porous Carbon Nanofibers from Electrospun Polyacrylonitrile/SiO_2 Composites as an Energy Storage Material. *Carbon* **2009**, *47* (14), 3346−3354.

(19) Sarkar, K.; Gomez, C.; Zambrano, S.; Ramirez, M.; de Hoyos, E.; Vasquez, H.; Lozano, K. Electrospinning to Forcespinning. *Mater. Today* **2010**, *13* (11), 12−14.

(20) Cremar, L.; Acosta-Martínez, J.; Villareal, A.; Salinas, A.; Wei, L.; Mao, Y.; Lozano, K. Multifunctional Carbon Nanofiber Systems Mass Produced from Water Soluble Polymers. *Chem. Fibers Int.* **2016**, *66*, 40−42.

(21) Guerin, K.; Fevrier-Bouvier, A.; Flandrois, S.; Simon, B.; Biensan, P. On the Irreversible Capacities of Disordered Carbons in Lithium-Ion Rechargeable Batteries. *Electrochim. Acta* **2000**, *45* (10), 1607−1615.

(22) Rochow, E. G. *The Chemistry of Silicon*; Pergamon Press, Oxford, 1973. p 1338.

(23) Feng, X.; Yang, J.; Lu, Q.; Wang, J.; Nuli, Y. Facile Approach to SiO_x/Si/C Composite Anode Material from Bulk SiO for Lithium Ion Batteries. *Phys. Chem. Chem. Phys.* **2013**, *15*, 14420−14426.

(24) Liu, N.; Wu, H.; McDowell, M. T.; Yao, Y.; Wang, C.; Cui, Y. A Yolk-Shell Design for Stabilized and Scalable Li-Ion Battery Alloy Anodes. *Nano Lett.* **2012**, *12* (6), 3315−3321.

(25) Wu, H.; Zheng, G.; Liu, N.; Carney, T. J.; Yang, Y.; Cui, Y. Engineering Empty Space between Si Nanoparticles for Lithium-Ion Battery Anodes. *Nano Lett.* **2012**, *12* (2), 904−909.

(26) Dirican, M.; Yanilmaz, M.; Fu, K.; Yildiz, O.; Kizil, H.; Hu, Y.; Zhang, X. Carbon-Confined PVA-Derived Silicon/Silica/Carbon Nanofiber Composites as Anode for Lithium-Ion Batteries. *J. Electrochem. Soc.* **2014**, *161* (14), A2197−A2203.

(27) Wang, Y.; Wen, X.; Chen, J.; Wang, S. Foamed Mesoporous Carbon/Silicon Composite Nanofiber Anode for Lithium ion Batteries. *J. Power Sources* **2015**, *281*, 285−292.

DOI: 10.1021/acsami.6b06051
ACS Appl. Mater. Interfaces 2016, 8, 29365−29372

(28) Dahn, J. R.; Zheng, T.; Liu, Y.; Xue, J. S. Mechanisms for Lithium Insertion in Carbonaceous Materials. *Science* **1995**, *270* (5236), 590−593.
(29) Liu, N.; Lu, Z.; Zhao, J.; McDowell, M. T.; Lee, H. W.; Zhao, W.; Cui, Y. A Pomegranate-Inspired Nanoscale Design of Large-Volume-Change Lithium Battery Anodes. *Nat. Nanotechnol.* **2014**, *9*, 187−192.

DOI: 10.1021/acsami.6b06051
ACS Appl. Mater. Interfaces 2016, 8, 29365−29372